Multiple Scattering of EM Waves by Spheres Part II—Numerical and Experimental Results

JOHN H. BRUNING, MEMBER, IEEE, AND YUEN T. LO, FELLOW, IEEE

Abstract—In [8], both low- and high-frequency solutions to the two-sphere problem were presented in a form suitable for efficient computer solution. Here, numerical results are presented using a method which has enabled the first appearance of reliable results for the scattered field from two spheres of radii larger than one wavelength and as large as ten or more. Radar cross sections (RCS) are computed for numerous configurations of two spheres of various materials. Results for scattering by three collinear spheres are also given. An experimental program was undertaken and is briefly described. Whenever possible, these results are compared with the theory. In all cases the agreement is excellent. Depolarization due to multiple scattering is also investigated, revealing some interesting effects and practical applications to scattering range calibration.

Introduction

THE SOLUTION to the electromagnetic (EM) scattering by two spheres has its roots as far back as 1935, but the complexity of the solution has thwarted efforts for numerical results for all but the smallest pair of spheres. A recent effort using the modern computer also failed to give reliable results for the same reason for spheres larger than $3\lambda/4$ in radius [9]. With the newly derived recursion relations, as given in [8], numerical computation becomes feasible for two spheres as large as 10λ in radius, of arbitrary material, and at any spacing, even in contact. It is also possible to extend the computation to three collinear spheres.

Little has been reported on the depolarization effect due to multiple scattering. This effect is studied for a few cases of two closely spaced spheres, with some revealing results. Such a study could find application in cross-polarization calibration in radar.

A fairly extensive experimental program was conducted to verify the theoretical results. The comparison has shown nearly perfect agreement in all cases. This is not accidental, since extreme care was exercised in planning and executing the experiments. Some of these are briefly discussed.

Manuscript received August 3, 1970. This work was supported in part by NSF under Grant GK4161 and in part by the Bendix Missile System Division under a Research Grant. This paper is based in part on a dissertation submitted by J. H. Bruning in partial fulfillment of the requirements for the Ph.D. degree.

J. H. Bruning was with the Antenna Laboratory, University of Illinois, Urbana, Ill. 61801. He is now with Bell Telephone Laboratories, Murray Hill, N. J. 07971.

Y. T. Lo is with the Antenna Laboratory, University of Illinois, Urbana, Ill. 61801.

Numerical Techniques

In the multipole expansion solution, the most difficult computational problem involves the calculation of the translation coefficients $A_{mn}{}^{m\nu}B_{mn}{}^{m\nu}$, [8, eqs. (22)–(25)]. Each of these coefficients is composed of a summation involving $1 + \max\{\nu,n\}$ terms, and each containing another coefficient $a(m,n,-m,\nu,p)$. Each one of $a(\cdot)$ is related to the product of two Wigner 3-j coefficients which are associated with the coupling of two angular momentum eigenvectors. Still, each of the Wigner coefficients involves multitudes of factorials [10]. This formulation of the translation theorem, as given by Stein [11] and Cruzan [12], was regarded as an elegant formulation since 3-j coefficients are extensively tabulated [1]. In terms of computation for the two or more sphere scattering problems, this is an impractical approach, since the number of 3-j coefficients needed is prohibitively large except for the smallest pair of spheres (radii much less than a wavelength). This was the approach taken recently by Liang and Lo [9]. To give some sort of feeling for the amount of computation involved using this technique, consider the case of computation of the scattered field from a pair of spheres of size $ka = 4$. This requires about ten radial modes in the multipole expansion of the scattered field. This means 2300 of the coefficients $a(m,n,-m,\nu,p)$ must be calculated! This is not a trivial task since the computation of a single coefficient $a(\cdot)$ involves as many as 156 factorials, the largest one being 41!. The situation gets rapidly out of hand as the spheres get larger. Generally, for a pair of spheres of size ka ($k = 2\pi/\lambda$, a = radius) approximately $N \approx ka + 3(ka)^{1/3}$ radial modes must be retained in the modal expansion. For this number of radial modes, the number of coefficients $a(\cdot)$ to be computed becomes rapidly large, as shown in Fig. 1. In addition, the problem of computing each $a(\cdot)$ becomes increasingly more difficult as N gets larger.

In [8], a recursive method was described for computing the coefficients $a(\cdot)$ which is highly efficient, and foremost, does not require the calculation of a single 3-j coefficient. This results in an astounding saving in computation time. For our previous example, $ka = 4$, the set of translation coefficients $A_{mn}{}^{m\nu}$ *and* $B_{mn}{}^{m\nu}$ can be generated 10^3 times more rapidly than by using the 3-j approach. The savings in time become even greater for larger spheres.

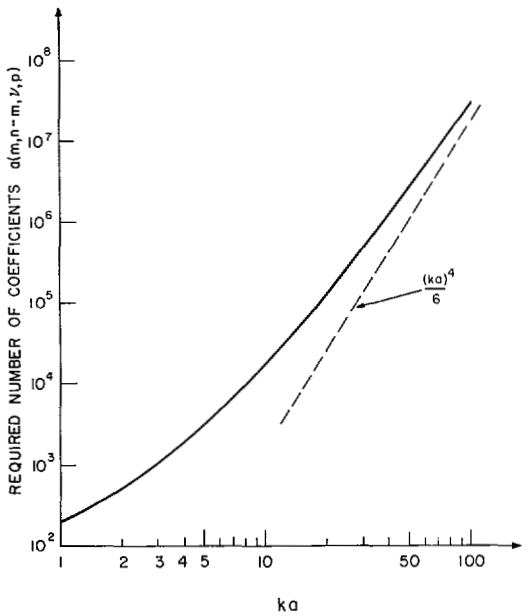

Fig. 1. Minimum number of coefficients $a(\cdot)$ required for calculation of multiple scattering by two spheres of size ka.

Next, we must solve for the multipole coefficients of each of the spheres which are coupled through the relation given in [8, eq. (7)] and which can be written in the matrix form:

$$\mathfrak{M} = \mathfrak{F} + \mathfrak{C}\mathfrak{M} \tag{1}$$

where $\mathfrak{M}$ is the column matrix forming the left-hand side (LHS) of [8, eq. (7)] from which the definition of the other elements follows. The solution is clearly

$$\mathfrak{M} = (I - \mathfrak{C})^{-1}\mathfrak{F}.$$

The matrix $(I - \mathfrak{C})$ may be inverted directly or $\mathfrak{M}$ may be determined by iteration. While the former method may always be applied, the latter requires that all eigenvalues of $\mathfrak{C}$ be of modulus less than unity. This method is, however, preferable as it tends to minimize error accumulation, requires less storage, and is more suited for computer solution. In terms of our previous example for two spheres $ka = 4$, the matrix inversion approach would require inversion of eleven 40×40 complex nonsymmetric matrices for one particular choice of parameters (sphere radii, separation, and material of each).

There are various iterative schemes available. The Gauss–Seidel iteration method was used almost exclusively instead of the slower Jacobi method which was used in [9]. It was rare to find a situation when this method did not converge. Convergence was for the most part rapid except when the spheres are in contact for the horizontal polarization. The iteration process is terminated when the final answer does not change within some prescribed amount.

With the multitudes of calculations involved, the question of numerical accuracy arises. This was checked in several ways. First, several programs were written at different times for different computers, in the Fortran II language in one case and Fortran IV in the others. There was agreement to no less than five of the six significant figures carried. Second, the reciprocity principle was exploited as a check. By illuminating the spheres at an incident angle α and observing the scattered field at an angle φ, we should obtain the same result as by illuminating at φ and observing at α. This allowed checking the endfire incidence program (which involves only the single azimuthal mode $m = 1$) with the general and broadside incidence programs. In all these cases tested, there was agreement to no less than four of the six places carried. Finally, the excellent agreement between the computed and experimental results places additional confidence in the results.

Before proceeding to the numerical results, some typical computer times are quoted and compared with the technique reported in [9]. It is difficult to make a direct comparison of the computation times between the present method and that in [9], since in the latter case only the first iteration toward the solution to the system of (1) was considered, whereas the present results were obtained by iterating as many times as necessary to obtain convergence to the true solution. The number of iterations required in some cases is very large. For example, in the case of large spheres ($ka > 15$) in contact at endfire illumination, the required number exceeds 40. For comparison, calculation of a single radar cross section (RCS) point for spheres with $ka = 4.19$ took about 11 min using the previously cited method and less than 1 s with the present method—the present method having performed an average of about six iterations, more near contact, less at large separation. The time factor between the two methods becomes rapidly larger as the sphere size increases. Calculations with the present program have been made for two spheres in contact at endfire incidence for $ka = 30$. At this value, the computer time is still quite reasonable, being only 40 s for a single point after performing about 50 iterations. The upper limit for sphere sizes depends on the price one is willing to pay for each point.

Numerical Results

It would be a difficult task to give a complete set of numerical results for scattering by two spheres because of the large number of parameters involved. To illustrate this, recall that for backscattering by a single sphere we have only the size and material to specify, whereas for two spheres we must specify not only the size and material of each, but also the separation between centers d, the incident wave vector $\boldsymbol{k}$ and its polarization.

Since measurements of RCS can be made with relative ease, this will constitute the major body of the numerical results. The backscattered far field is given by [8, eq. (8)] with $\theta = \pi - \alpha$ and $\phi = \pi$. Using this, we may compute the RCS from the definition

$$\sigma = \lim_{r \to \infty} 4\pi r^2 \mid E_s/E_i \mid^2.$$

In what follows, this is calculated for various configurations of two and three spheres. In nearly all RCS computations, experimental results are also shown for comparison, although the experimental procedures are not discussed until later. Unless otherwise stated, solid curves were computed using the multipole expansion (exact) technique, and dotted curves represent the experimental results. The theoretical curves were plotted by computer in a manner similar to that described in [8]. By plotting the theoretical curves to the same size and scale as the experimental results, the latter could be transferred simply by tracing. This explains the somewhat unusual scales used.

Broadside Incidence—Variable Separation

Fig. 2 shows the broadside RCS of a pair of identical metallic spheres for $\gamma = \pi/2$, normalized to σ_a, the RCS of sphere A alone for $ka = 4.19$ and $ka = 6.246$. The agreement is remarkably good with the exception of an apparent scale shift near contact. This is an experimental error associated with one of the suspension techniques and is explained elsewhere [13]. The coupling which is manifested by the oscillations about the line $4\sigma_a$ (6 dB) is nearly negligible for $d/a > 6$. This has a simple interpretation in terms of geometric optics as explained in [8]. Similar results were calculated and measured for a pair of dielectric spheres and adjacent dielectric and metal spheres, but the coupling is in general much weaker because of the low reflectance, in the optical sense, of an air dielectric interface.

Endfire Incidence—Variable Separation

RCS calculations and experimental measurements for the endfire cases are shown in Figs. 3 and 4. As in the other cases, experimental and theoretical results are normalized to the RCS from the front sphere alone. Fig. 3 shows the cases of identical metallic spheres for $ka = 7.41$ and 11.048; the former case was chosen for comparison with the experimental results of Angelakos and Kumagai [14] which are indicated by the squares. These results indicate very little coupling for $d/a > 5$.

The RCS of two identical dielectric spheres at endfire is shown in Fig. 4(a) for $ka = 7.44$. Here we see that the interaction between the spheres persists for larger values of kd than for the case of metallic spheres nearly the same size as in Fig. 3(a). The stronger coupling in this case may be due to a focusing effect from the front sphere. In the adjacent curve, Fig. 4(b), we have a metallic sphere behind a dielectric sphere, both about the same size. The large return at and near contact may be interpreted as due to rays focused by the front dielectric sphere, reflected by the metallic sphere and refocused by the dielectric sphere back to the observer, analogous to placing a mirror behind a lens near its focal point. The same enhancement for this geometry and the same spheres was also observed both experimentally and theoretically at several other frequencies. It is interesting to note that the optical paraxial focus of the dielectric sphere is positioned at a distance of $0.3a$ from the back surface of the sphere.

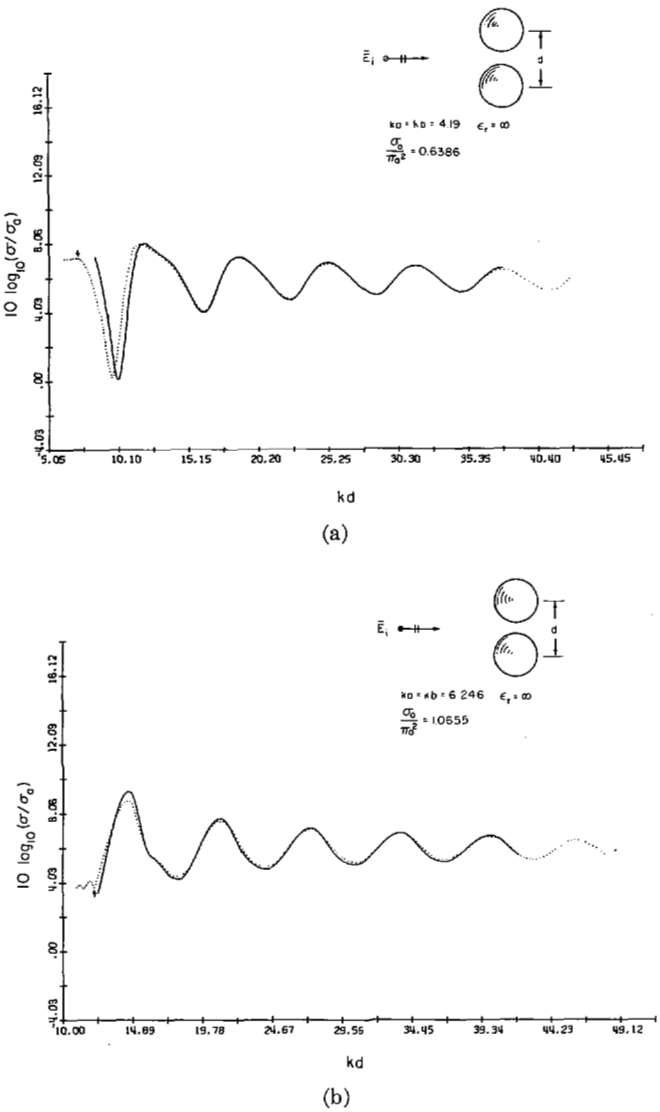

Fig. 2. RCS of two equal metallic spheres at broadside incidence. (a) $ka = 4.19$. (b) $ka = 6.246$. Modal approach (—) and experiment (• • •).

Variable Angle of Incidence—Fixed Separation

In Fig. 5, the aspect angle, or angle of incidence α is the independent variable while the spacing remains fixed. In these two cases the spheres are in contact as the aspect changes. Recall that at contact the coupling is strongest, requiring the most iterations. Again, the difference between measured and experimental results is extremely small. We note also, as previously mentioned, the large enhancement of the radar return when the dielectric sphere is in front of the metallic one, even though the sizes are different from those in Fig. 4(b).

Bistatic Cross Sections

The multipole coefficients for the two spheres, or any scatterer, clearly depend on the angle of incidence of the plane wave and not the point of observation. Hence,

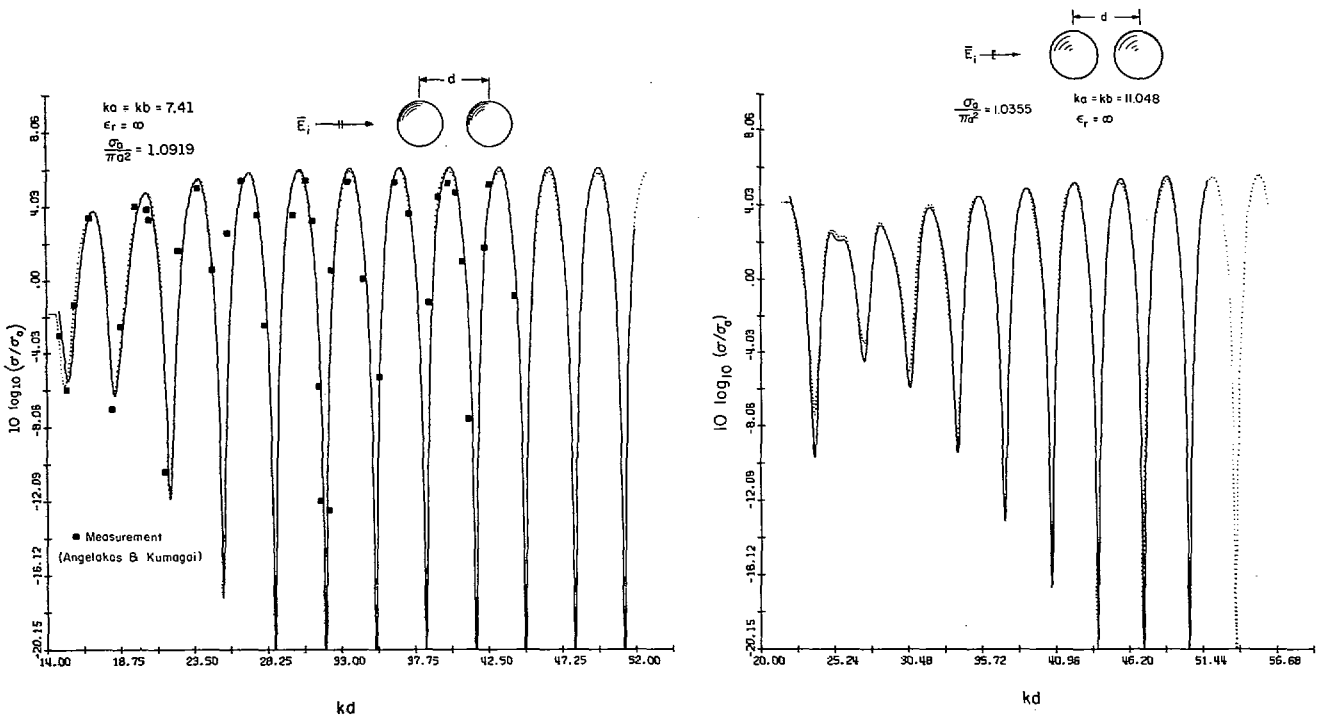

Fig. 3. RCS of two equal metallic spheres at endfire incidence. (a) $ka = 7.41$. (b) $ka = 11.048$. Modal approach (—) and experiment (•••).

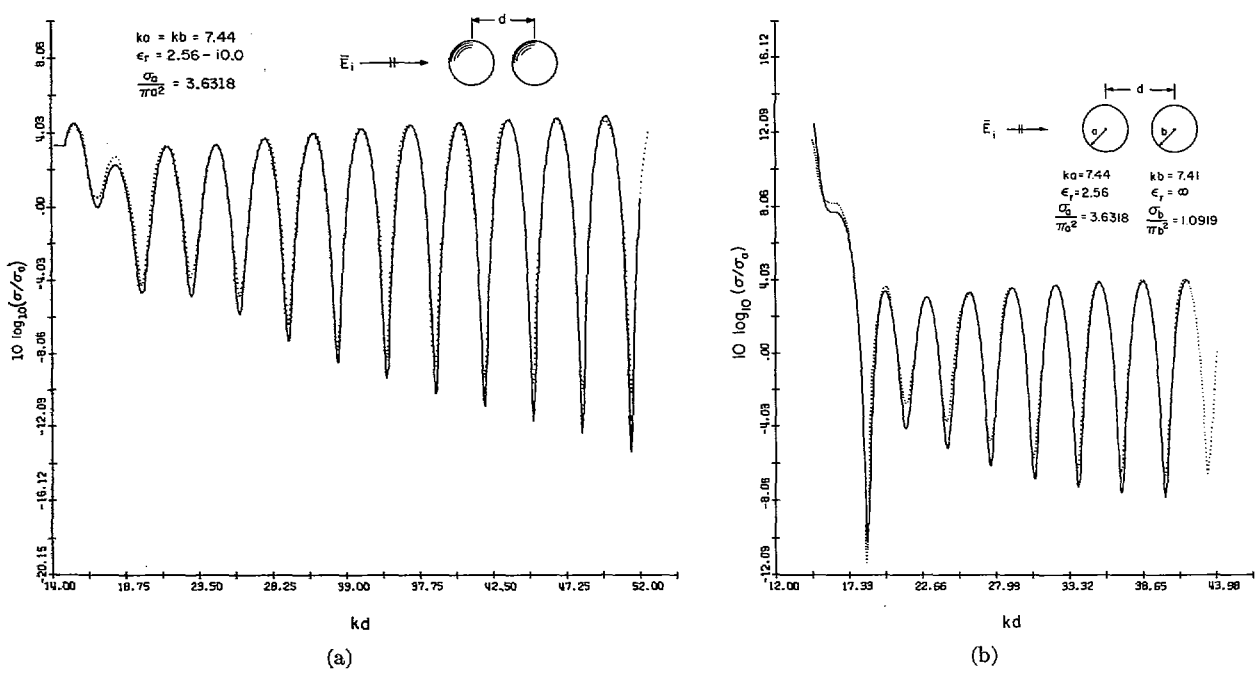

Fig. 4. RCS of spheres at endfire incidence. (a) Two dielectric. (b) One dielectric and one metallic. Modal approach (—) and experiment (•••).

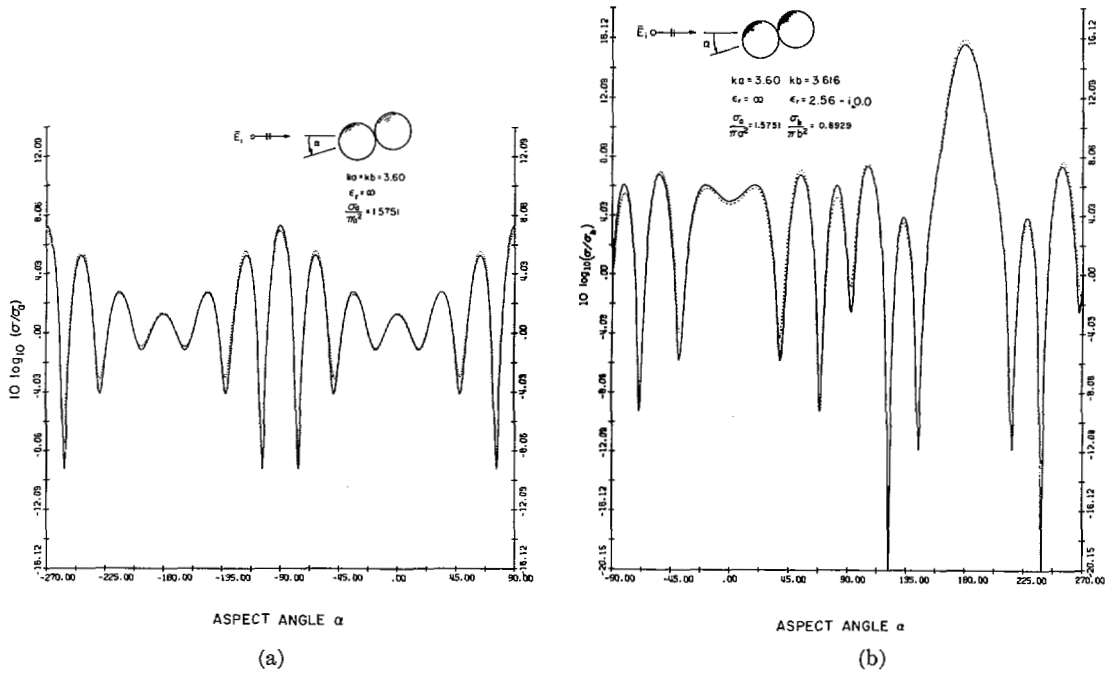

(a) (b)

Fig. 5. RCS of spheres in contact versus aspect angle. (a) Two metallic. (b) One metallic and one dielectric. Modal approach (—) and experiment (•••).

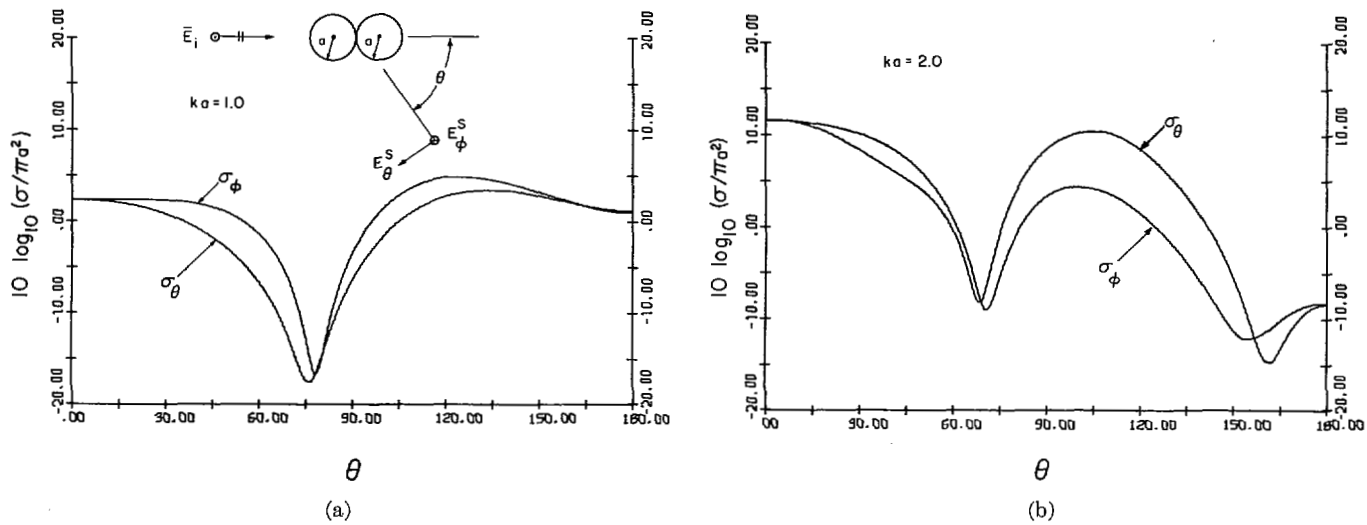

(a) (b)

Fig. 6. Normalized bistatic cross section in two principal planes for two spheres in contact at endfire illumination using modal solution. (a) $ka = 1.0$. (b) $ka = 2.0$.

once the coefficients $A_E(m,n)$, $A_H(m,n)$, $B_E(m,n)$, $B_H(m,n)$ are calculated, it is a simple matter to find the scattered field in any direction. Two such examples are considered in Fig. 6 where σ_θ and σ_ϕ corresponding to E_θ and E_ϕ, respectively, have been computed for $ka = 1$ and 2. We see, as expected, that these two cross sections coincide in the two directions of axial symmetry.

Depolarization Due to Multiple Scattering

From [8, eq. (8)] we can see that if the incident EM field is linearly polarized in one of the two principal planes ($\gamma = 0, \pi/2$), there is no depolarization of the backscattered field regardless of sphere sizes, material, or angle of incidence α. If the incident field is polarized in some other direction, both incident field components will be present, each of which in general scatter a different field, thus depolarizing the scattered field. Beckmann [2] defines a polarization factor (call it P) as the quotient of the horizontal and vertical components of the electric field under consideration. Hence a horizontally polarized field has a polarization factor of infinity, and for vertical polarization it is zero. All complex values of P represent elliptical polarization in general, with a right rotational sense if Im $\{P\} < 0$ and a left rotational sense if

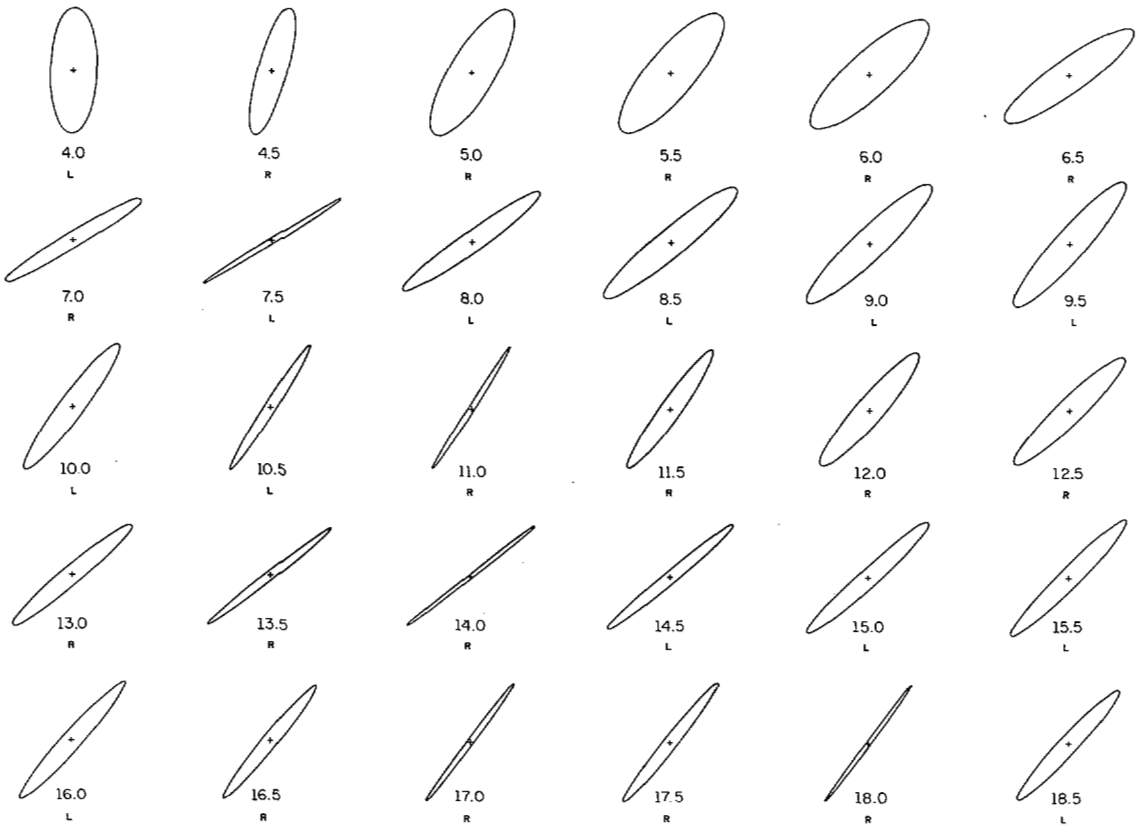

Fig. 7. Polarization ellipses of backscattered field of two equal metallic spheres $ka = 2.0$ versus separation kd from broadside incident plane wave linearly polarized at 45°.

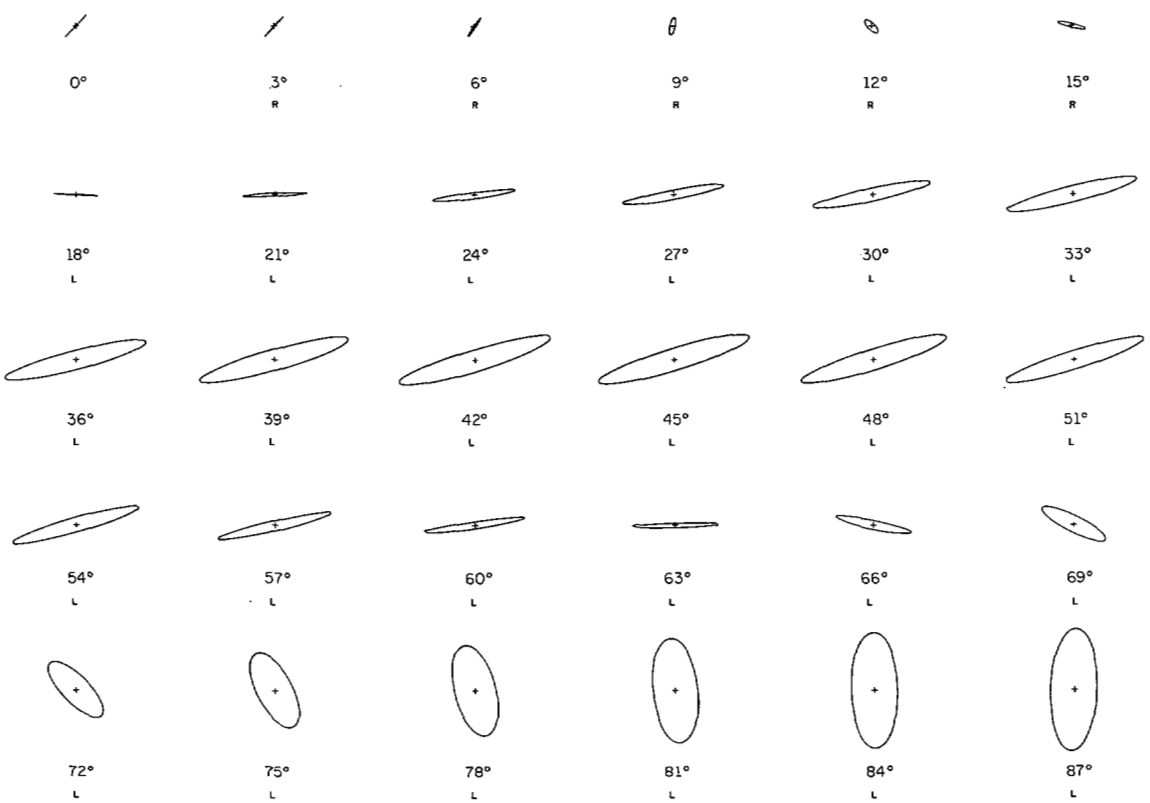

Fig. 8. Polarization ellipses of backscattered field of two equal metallic spheres $ka = 2.0$ in contact versus aspect angle from incident plane wave linearly polarized at 45°.

Im $\{P\} > 0$. Circular polarization is described by the values $\pm i$. If now a scattered wave has the same polarization factor as the incident wave, then the scatterer has not depolarized the incident wave. A depolarization factor D is then defined as: $D = P_s/P_i$. Hence $D = \pm 1$ when there is no depolarization. If we consider only the backscattered field, then by symmetry we know that an isolated sphere cannot depolarize an incident plane wave regardless of incident polarization. The same would also apply to any two spheres if there were no coupling between them. Therefore, in the absence of symmetry, the depolarization of the backscattered field from two adjacent spheres is an indication of the degree of the coupling between the spheres. Consider first the case of two identical spheres at broadside incidence. As we said previously, there will be no depolarization at $\gamma = l\pi/2$, where l is any integer. Consider the intermediate cases where $\gamma = (2l - 1)\pi/4$; then depolarization of the backscattered field is expected. The depolarization will be strong for close spacing and weak for large.

Fig. 7 shows polarization ellipses of the broadside backscattered field from two identical perfectly conducting spheres $ka = 2$, illuminated by a plane wave with $\gamma = \pi/4$, ($P_i = 1$). The number under each ellipse is the center separation kd and the letters L and R indicate the sense of polarization. At contact ($kd = 4$), strong depolarization is evident. As the sphere separation increases, the ellipse orientation oscillates about the direction of the incident $\boldsymbol{E}$ vector; the ellipse itself contracts and expands, undulating and changing the sense of polarization in the process, and eventually converging to a 45° line corresponding to no depolarization. It is rather fascinating to portray such a complex scattering process through the use of depolarization.

The depolarization effects are perhaps even more vividly seen in Fig. 8 where polarization ellipses are shown for the backscattered field of the same two spheres this time as they rotate in contact ($\alpha = 0 \rightarrow 87°$). Here, starting at endfire where there is no depolarization (because of symmetry), we see that the major axis of the ellipse swings from +45° to about 190° and then back to approximately 90° with wide variations in the amplitude. Several other cases of this type were investigated for different ka, with the interesting result that some cases exhibited a backscattered field at particular angles with nearly perfect circular polarization ($D \approx \pm i$).

As final examples, we compute the cross-polarized RCS normalized to πa^2 for the two examples considered previously. The transmitted (incident) field is polarized at $\gamma = 45°$ and the received at 135°. Hence, if there were no coupling, we would receive nothing at this orthogonal polarization as with an isolated sphere. Results of this type for the broadside case are shown in Fig. 9(a). The decrease in the cross-polarized RCS is quite rapid as kd is increased. This is to be expected since the coupling is generally related to the ratio d/a which changes more rapidly for small spheres for the same interval in kd.

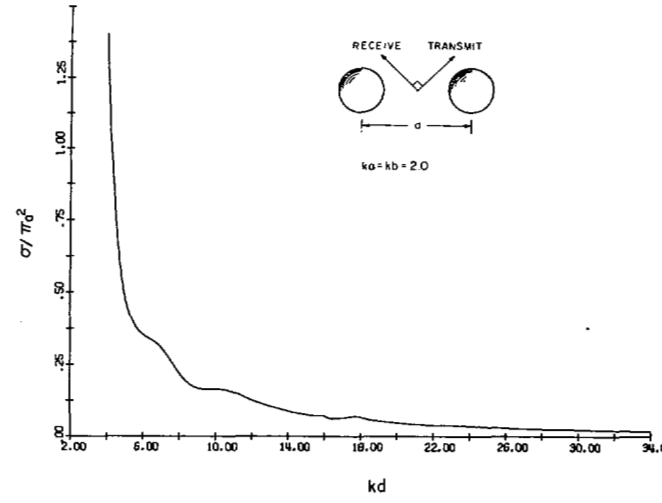

(a)

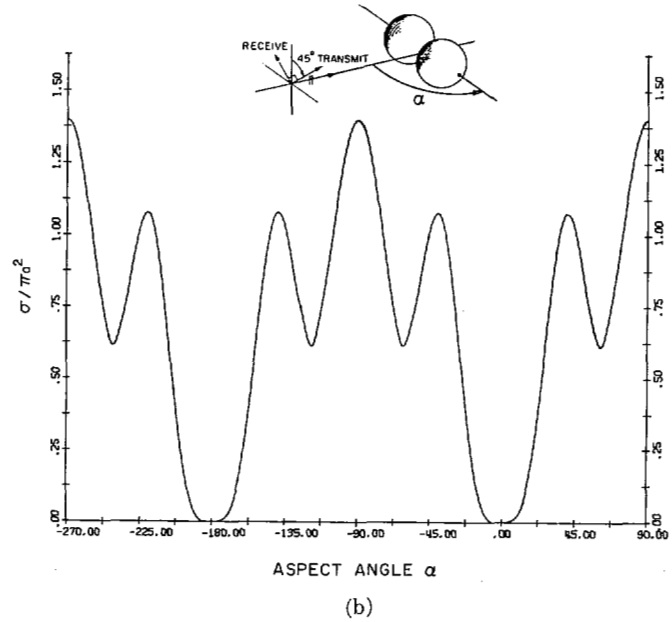

(b)

Fig. 9. Cross-polarized RCS of two equal metallic spheres $ka = 2.0$. (a) Versus separation. (b) In contact versus aspect angle.

For large spheres, this behavior may be very simply predicted by geometric optics as shown in [8].

The cross-polarized RCS for two equal spheres in contact as their aspect angle changes is shown in Fig. 9(b). As we expect, there is no cross-polarized return for the aspect angles 0 and π. It was suggested by Knott [3] that two spheres in either of these configurations might serve as a new means of calibration for cross-polarized RCS measurements. Another application would be the calibration of circularly polarized radars which transmit and receive the same sense of circular polarization and as such reject the return from symmetrical targets, such as rain clutter (which assumes no multiple scattering). The large number of parameters in the two-sphere system would allow calibration of such a radar over nearly any desired dynamic range.

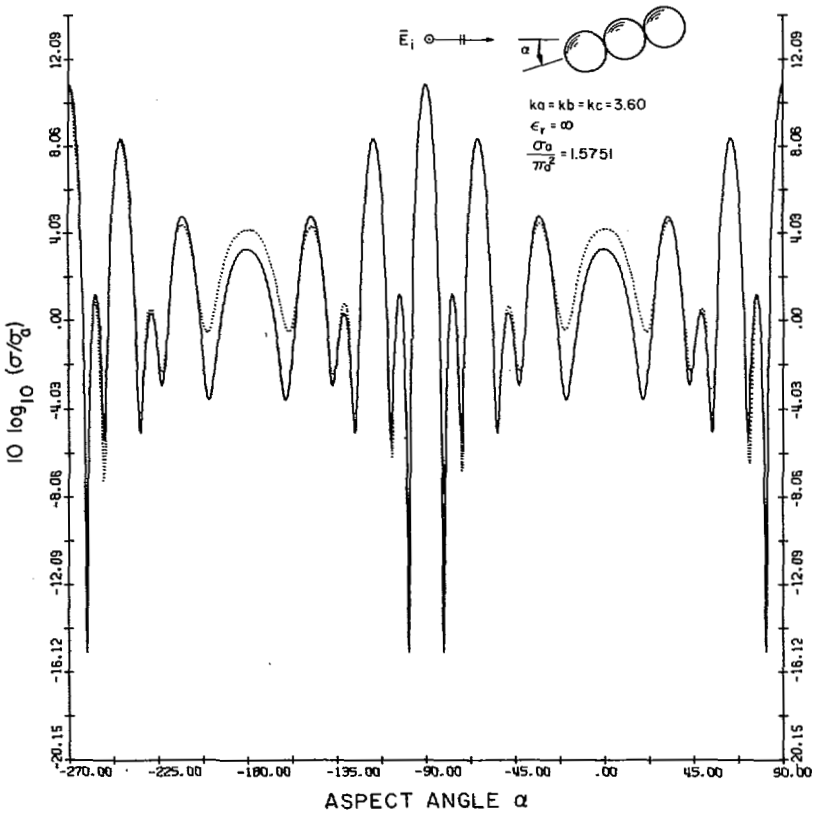

Fig. 10. RCS of three equal metallic spheres in contact versus aspect angle. Modal solution (—) and experiment (•••).

Miscellaneous Results

The extinction or total scattering cross section is a frequently discussed quantity in single body scattering theory since it is so simply related to the forward scattered field of the object [4]. In the case of scattering by a single lossless sphere, the normalized extinction cross section approaches asymptotically the value 2 as $ka \to \infty$; i.e., the cross section approaches twice its geometric area. We would expect that in the absence of multiple scattering, the total scattering by two bodies would be the sum of the total scattering by each, regardless of orientation. With multiple scattering it is no surprise that the total cross section varies with changes in the configuration of two spheres. As separation is increased, the total cross section oscillates about and eventually converges to the value which is the sum of the total cross sections of the two isolated spheres. No such general statements can be made concerning other parameter changes.

The rather interesting phenomena of resonance scattering by isolated dielectric spheres also deserves some attention in relation to multiple scattering. When $\epsilon_r^{1/2} \gg 1$, one finds very strong peaks in the scattering by a single sphere [5]. The first peak occurs quite reliably at $ka = \pi(1 - \epsilon_r^{-2})/\epsilon_r^{1/2}$ and is due to the very small value in the denominator of the first magnetic dipole coefficient [4]. Now consider Rayleigh scattering for two small spheres. In this case, one may solve for the multipole coefficients explicitly. If, however, the spheres are in close proximity, the resonant phenomena can be drastically altered. This can be understood in terms of the matrix representation of (1). In the case of one or both spheres near resonance, $\mathfrak{C}$ will be large, implying that $\mathfrak{M}$ is not given by a small perturbation of $\mathfrak{F}$. This also indicates that (1) cannot be solved by iteration.

One such case of "resonant multiple scattering" was investigated numerically for two identical lossless dielectric spheres with $\epsilon_r^{1/2} = 50$. The first resonance for the isolated sphere occurs at $ka = 0.0628068$. The normalized RCS of one of these spheres at this value of ka is 2280! As indicated earlier, multiple scattering effect by two spheres is usually small when the spheres are separated by several diameters ($d/a > 6$); however, for this case, the interaction is considerable even for $d/a \approx 50$. It would indeed be interesting to investigate this experimentally, even for a single resonant sphere.

There are many other results that could be cited but they are too numerous to be included here. They may be found in [13].

It is curious that the history of the problem does not include (to the authors' knowledge) the solution to the simpler problem of scalar or acoustic scattering by two spheres. This problem has been solved [13] and it will appear in a future publication.

Three-Sphere Problem and Some Numerical Results

The generalization of the results for electromagnetic scattering by two spheres to the case of three [13], [15] is quite straightforward but tedious. No attempt was made to obtain numerical results for the very general

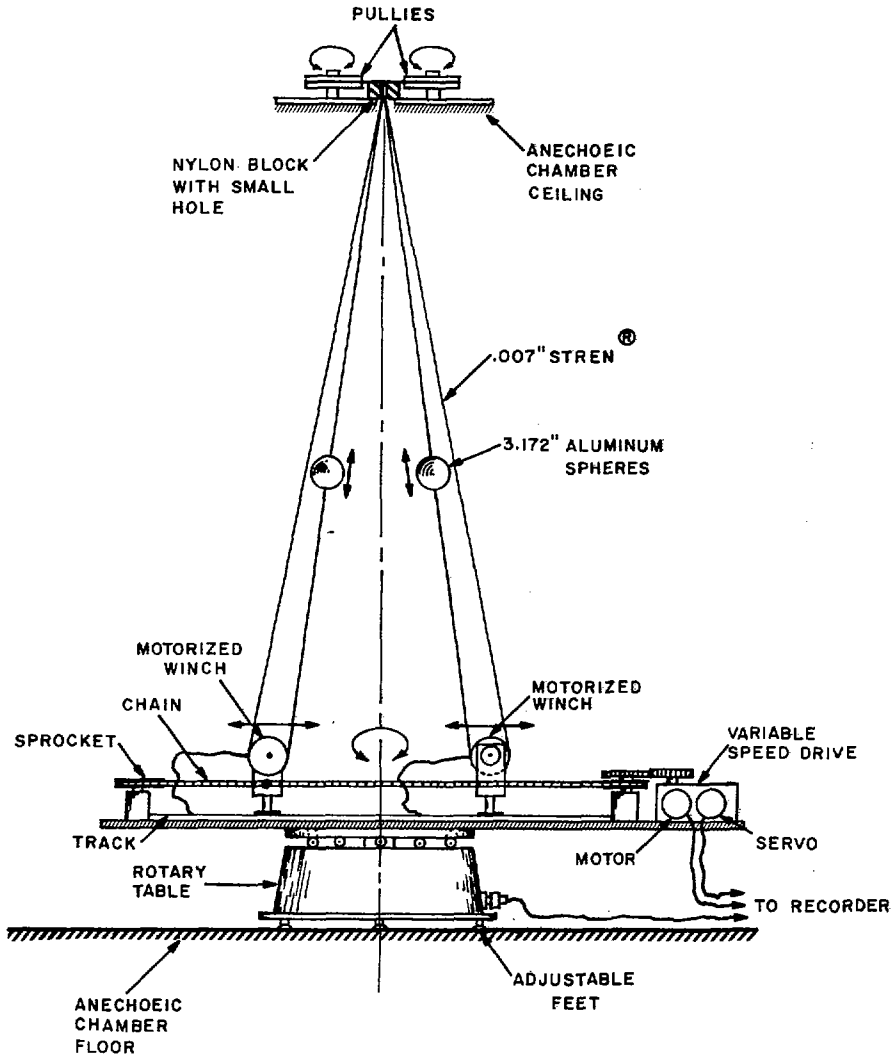

Fig. 11. Suspension technique for all orientations of two spheres.

case of three spheres, but it is relatively simple to consider a collinear array of three spheres of equal size, equally spaced. For this case, two sets of translation coefficients are needed, namely, $A_{mn}^{m\nu}(d)$, $B_{mn}^{m\nu}(d)$ and $A_{mn}^{m\nu}(2d)$, $B_{mn}^{m\nu}(2d)$. When these are used and the boundary conditions satisfied, we are led to a system of six coupled sets of equations of a form similar to [8, eq. (7)]. Fig. 10 shows numerical and experimental results for three equal metallic spheres in contact as the aspect angle α is changed. The agreement is excellent except near endfire. Further numerical results and measurements with various combinations of three spheres (dielectric and metallic) showed a generally high sensitivity to sphere alignment at and near endfire. Misalignment of sphere A or C could be easily detected as an asymmetry in the recorded scatter pattern; however, if the center sphere were positioned slightly high or low with respect to the other two, then the pattern would still retain its symmetry. This type of misalignment (if indeed there was any) could not be detected at the time of the measurement.

Consideration and Procedure in Experiment

In view of the complexity of the solution, it is desirable to have experimental verification of the theoretical results. A practical quantity for measurement is the RCS. Through an inter-university cooperative organization, (CIC), we were fortunate to have the permission to use the excellent scattering measurement facilities of the Radiation Laboratory, University of Michigan. A detailed description of the range may be found in [6].

In contrast to the experiment reported in [14], [16], the present measurements were made for continuously varying sphere spacings or incident angles by means of servos. To keep the unwanted background scattered energy to a minimum, it was decided to support the spheres with thin suspension lines. This was possible only if the spheres were not excessively heavy. For this reason, the following different kinds of spheres were used: 3-in and 5-in hollow aluminum, 3-in Rexolite, and less than $1\frac{1}{2}$-in copper-plated steel (ball bearing). The

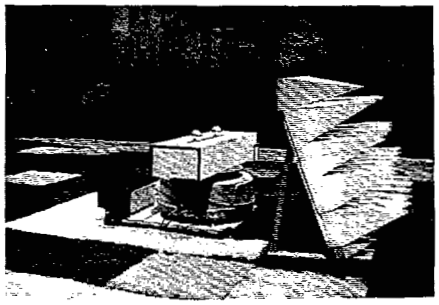

(a)

(b)

Fig. 12. Suspension technique showing spheres. (a) In lowered position for balancing of chamber. (b) In raised aligned position ready for measurement.

commercially available monofilament line Stren® was used; it has a high tensile strength before plastic stretching. The 2 lb line is 0.005-in in diameter; it was found to introduce a signal 40 dB below that from the two spheres under test [7]. Several suspension techniques were actually used [13], but only one is described in the following.

It is obviously desirable to have the capability of making all adjustments and alignment of the spheres from outside the anechoeic chamber, including a method for withdrawing the spheres to balance the system. To this end, a system was constructed, as shown schematically in Fig. 11. As seen, the rotary table provides for aspect angle changes; another motor and servo allow the spheres to be separated at will, and small motorized pulleys allow both spheres to be moved up and down independently. All these motions can be controlled from outside the chamber. The unit is covered with microwave absorbing material to minimize extraneous scattering.

® Registered trade mark of E. I. duPont De Nemours.

Measurements for any of the configurations could be made quite rapidly with this system. Since a variable ratio drive mechanism was used for separation of the spheres, a horizontal scale expansion or compression feature for the recorded RCS pattern was available. Fig. 12(a) shows the two spheres withdrawn below the absorbing barrier in position for the balancing of the system, and Fig. 12(b) shows the same spheres raised and aligned in position for the start of a measurement.

The results consistently showed excellent agreement with the theory, indicating that the return from supporting structure and suspension lines was indeed small. This of course must also demonstrate an overall superb quality of the microwave equipment and the chamber itself at the Radiation Laboratory.

Acknowledgment

The authors wish to thank Prof. R. E. Hiatt of the Radiation Laboratory at the University of Michigan for making possible the use of their excellent scattering facility and E. F. Knott and C. Grabowski for their assistance. Without this help, the investigation would never have been as complete as in the present form.

References

[1] M. R. Rotenberg, R. Bivins, N. Metropolis, and J. K. Wooten, Jr., *The 3-j and 6-j Symbols*. Cambridge, Mass.: M.I.T. Press, 1959.
[2] P. Beckmann, *The Depolarization of Electromagnetic Waves*. Boulder, Colo.: Golem Press, 1968.
[3] E. F. Knott, private communication, Dec. 1968.
[4] D. S. Jones, *The Theory of Electromagnetism*. New York: Pergamon, 1964.
[5] G. W. Kattawar and G. N. Plass, "Resonance scattering from absorbing spheres," *Appl. Opt.*, vol. 6, 1967, no. 9, pp. 1549–1554.
[6] E. F. Knott, "An indoor radar scattering range," Rome Air Development Center, Rome, N. Y., Tech. Doc. Rep. RADC-TDR-64-25, ASITA Doc. AD 601 365, Apr. 1964.
[7] C. C. Freeny, "Target support parameters associated with radar reflectivity measurements," *Proc. IEEE*, vol. 53, Aug. 1965, pp. 929–936.
[8] J. H. Bruning and Y. T. Lo, "Multiple scattering of EM waves by spheres part I—multipole expansion and ray-optical solution," this issue, pp. 378–390.
[9] C. Liang and Y. T. Lo, "Scattering by two spheres," *Radio Sci.*, vol. 2, 1967, no. 12, pp. 1481–1495.
[10] A. R. Edmonds, *Angular Momentum in Quantum Mechanics*. Princeton, N. J.: Princeton Univ. Press, 1957.
[11] S. Stein, "Addition theorems for spherical wave functions," *Quart. Appl. Math.*, vol. 19, 1961, no. 1, pp. 15–24.
[12] O. R. Cruzan, "Translational addition theorems for spherical vector wave functions," *Quart. Appl. Math.*, vol. 20, 1962, pp. 33–40.
[13] J. H. Bruning and Y. T. Lo, "Multiple scattering by spheres," Antenna Lab., Univ. Ill., Urbana, Tech. Rep. 69-5, 1969.
[14] D. J. Angelakos and K. Kumagai, "High-frequency scattering by multiple spheres," *IEEE Trans. Antennas Propagat.*, vol. AP-13, Jan. 1964, pp. 105–109.
[15] R. K. Crane, "Cooperative scattering by dielectric spheres," M.I.T. Lincoln Lab., Lexington, Mass., Tech. Note 1967-31, 1967.
[16] J. Mevel, 'Contribution de le diffraction des ondes electromagnetiques par les spheres," *Ann. Phys.* (Paris), 1960, pp. 265–320.